THE APPLICATION OF ENDOSCOPE AND IMAGE PROCESSING FOR DETERMINING REMAZOL RED DYE CONCENTRATION IN WATER SAMPLES

Nazatul Akmal Nazibudin, Mohamad Faiz Zainuddin*, Tengku Nur Adriana Tengku Nazruddin, Rona Techly Deny, Khairunnisa Kadaruddin

Department of Environment, Faculty of Forestry and Environment, University Putra Malaysia, 43400 Serdang, Selangor, Malaysia

*Corresponding author
z_faiz@upm.edu.my

Graphical abstract

Detection of dye samples with commercial colorimeter

Detection of dye samples with a digital endoscope

Abstract

Remazol dyes are widely used in textile industry, which are then discharged to the environment as waste products. Studies on bioremediation and decolorization of dye waste normally employ expensive spectrometers or colorimeters. This study proposes a low-cost procedure to determine the concentration of Remazol red dye with the use of a digital endoscope and image processing technique. The concentration of Remazol red dye considered in this study ranges from 0.001 to 0.700 g/L. An endoscope is used to capture digital images of dye samples. Reg-green-blue (RGB) images of the samples are converted to grayscale images, which are then converted to a mean grayscale index (MGI). The MGI is then calibrated with real concentration of dye samples. Three calibration curves were developed for three different ranges of dye concentration of 0.001- 0.010 g/L, 0.020 – 0.100 g/L, and 0.100 – 0.700 g/L, with a coefficient of determination (R^2) of 0.961, 0.9793, and 0.9903, respectively.

Keywords: Remazol dye, endoscope, Image Processing, RGB, grayscale

Abstrak

Pewarna Remazol diguna secara meluas dalam industri pakaian yang akan dilepaskan ke alam sekitar sebagai bahan buangan. Kajian melibatkan bioremediasi dan penyahwarnaan pewarna buangan biasanya menggunakan spectrometer atau kolorimeter yang mahal. Penyelidikan ini mencadangkan satu prosedur kos rendah untuk menentukan kepekatan pewarna merah Remazol dengan menggunakan sebuah endoskop digital sebagai alat pengesan cahaya dan teknik pemprosesan imej. Kepekatan pewarna merah Remazol yang digunakan dalam penyelidikan ini berjulat daripada 0.001 kepada 0.700 g/L. Endoskop digunakan untuk menangkap gambar digital sampel pewarna. Imej merah-hijau-biru (RGB) sampel tersebut ditukar kepada skala kelabu yang kemudian ditukarkan kepada indeks purata skala kelabu (MGI). MGI ditentukur dengan kepekatan asal sampel pewarna. Tiga kurva kalibrasi dibangunkan daripada data yang diukur untuk tiga julat kepekatan pewarna 0.001- 0.010 g/L, 0.020 – 0.100 g/L dan 0.100 – 0.700 g/L, masing-masing dengan pekali penentuan (R^2) 0.961, 0.9793 dan 0.9903.

Kata kunci: Pewarna Remazol, endoskop, pemprosesan imej, GRB, skala kelabu

1.0 INTRODUCTION

Color is an important physical parameter of water quality other than turbidity, temperature, taste, odor, and solids [1]. It is also an important indicator of water pollution [2]. Natural water is essentially colorless with a slight blue tint [3]. Color in water can be caused by many factors such as organic matters, metals, and industrial wastes [4, 5]. The apparent color of water is the result of colloidal suspensions that can be isolated with filtration and often attributed to iron or dissolved plant tannins. True color of water, on the other hand, is due to dissolved chemical and organic substances that cannot be isolated with filtration [1,6].

Many modern standard methods for determining the color of water and wastewater such as Method 8025, Method 2120B/C (EPA110.2/3), and ASTM D 1209 are adopted from the Hazen method. These methods examine comparisons of spectrophotometer absorbance readings between water samples and platinum-cobalt solution at a specific wavelength between 410 nm and 465 nm. A spectrophotometer or a colorimeter is commonly used as an instrument to determine the color of water, since people's perception of color can be subjective and lacks sensitivity [7, 8].

However, the price of de-facto standard scientific instruments such as spectrometers, colorimeters, and turbidimeters can be prohibitively expensive for low resource communities to carry out effective and continuous natural and wastewater quality monitoring [9, 10]. As reported in [11], the price of a table-top UV-Vis spectrophotometer (Cary 60 UV-Vis) can go up to USD30,000, while the prices of portable spectrophotometers (Hach) range from USD2000 to USD8000. The price of these instruments can be more expensive if one includes the cost of shipping, foreign exchange, sales fee or commissions, taxes, duties, and other factors.

For that reason, many recent studies in sensors and instrumentations focus on developing low-cost instruments and procedures to accurately determine the level of turbidity [12, 13, 14, 15] and color [11, 16, 17]. These innovations take advantage of inexpensive and widely available electronic and optical components such as LEDs, light sensors, printed circuit boards (PCB), microcontrollers, and Arduino modules to minimize the cost. Containers housing these components as well as water sample holders or cuvettes can be fabricated from various economical materials such as polylactic acid (PLA), nylon block, and corrugated papers. Mobile applications and open-source technology are used to process and analyze sampling data to obtain the desired measured values [18]. Besides being used as scientific field instruments, these low-cost devices can also be used for education and teaching purposes.

Past studies have shown that industries such as pharmaceuticals, cosmetics, textile, and food utilize thousands of synthetic azo dyes in their manufacturing processes, which are then discharged into water as waste products [19]. Even at low concentrations, dye wastes and their degradation products can pose health threats to living organisms including humans [20, 21]. Among widely used dyes in textile industries are Remazol dyes, and they are subjects of interest in bioremediation of dye waste [22, 23]. In bioremediation studies, UV-Vis is commonly used to determine the percentage of decolorization of dye waste.

This study attempts to determine the concentration of Remazol red dye solution in water samples with a digital endoscope and an image processing technique. This endoscope is considered in this study because it is inexpensive, and its small diameter allows it to be inserted inside a small opening of standard sample cuvette which holds the water samples. The main function of the endoscope is to detect light by capturing digital images of the water samples. The amount of light that enters the endoscope will impact the pixel value distribution of digital images obtained by the endoscope. On the other hand, image processing is used for image conversion and data analysis. This paper covers the procedure to acquire images of water-red dye mixture samples with an endoscope and the fitting model relating the pixel value and the concentration of the samples.

2.0 METHODOLOGY

2.1 Beer-Lambert and Fresnel's Law

Many instruments to quantify water turbidity and color are based on Beer-Lambert law. Beer-Lambert law deals with the absorbance and reflectance of light by a medium such as a body of water which gives the medium (water) its apparent color. The suspended particles inside a body of water are mainly responsible for blocking and redirecting light from transmitting through water. With the absence of suspended particles, which is the case with pure or very clean water, light transmission is largely uninterrupted or with little scattering. Hence, pure or very clear water is considered colorless. Light scattering, absorption, and transmissions are dependent on many factors such as the size, shape, and composition of suspended particles as well as the wavelength of the incident light [24].

Besides light absorption and reflectance by a body of water, since 1950s, there has been a large number of studies dedicated towards understanding how suspended particles interact with light at the surface [25]. One recently published paper attempted at finding the relationship between refractive index and concentration of dye. The paper discovered that the refractive index of Brilliant Blue dye solution increases with increasing dyeconcentration [26]. The refractive index,

according to Fresnel's equation, describes the amount of light reflected and transmitted into a medium when light is incident at the boundary between different media. According to Fresnel's law, normal incidence reflection at the interface between air and water sample is given as follows [27]:

$$R = \frac{(n_a - n_s)^2}{(n_a + n_s)^2} \qquad (1)$$

where n_a and n_s are the refractive indices of air and the sample, respectively. The refractive index of air is assumed to be 1, while the refractive index of dye solution depends on types of dye, dye concentration, and wavelength. As the value of n_s increases, the value of R is expected to increase as well due to increasing refractive-index mismatch between air and the sample.

2.2 Preparation of Remazol Red Dye Samples

Remazol red dye was imported and procured from Germany. The water-soluble dye came in powder form. Red dye solutions were prepared by dissolving a specific amount of red dye powder in one mixture; solutions were prepared ranging from 0.001 g/L to 3.0 g/L, to determine the detection limit of the endoscope (Figure 1). The temperature of the samples was maintained at ambient temperature during the measurement. It was noticed that the color intensity or the saturations of the samples increases with increasing concentration. The measures of absorption and reflectance of the dye samples were obtained with a UV-Vis spectrophotometer (SHIMADZU UV-3600) at the Faculty of Science, Universiti Putra Malaysia (UPM).

2.3 Fabrication of cuvette holder

A lightproof cabin was fabricated to house the cuvette (Figure 2 and 3). The design came with a lid with a tiny hole to allow the endoscope to be inserted inside the cabin; but without allowing light to enter the cabin through the hole. The material used to fabricate the cabin was corrugated paper, which was then covered with black tape on the outside to ensure that the entire wall is opaque to light [15, 28].

(a) 0.001 g/L – 0.01 g/L

(b) 0.02 g/L – 0.2 g/L

(c) 0.3 g/L – 3.0 g/L
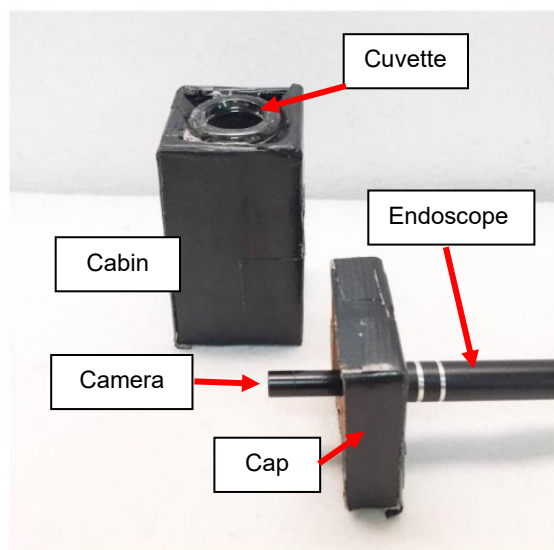
Figure 1 Remazol dye-water mixture samples
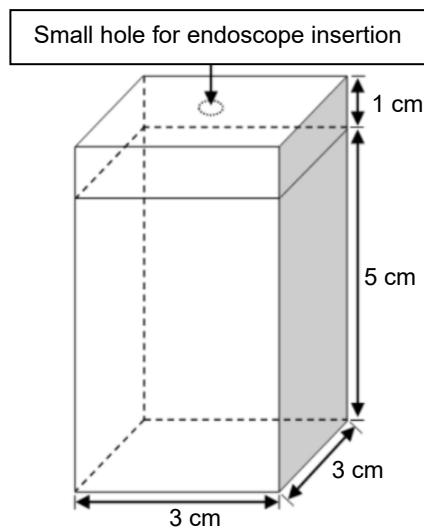
Figure 2 The cabin

Figure 3 The dimension of the cabin

On the other hand, the inside wall of the cabin is painted white to make sure the samples are visible to white to make sure the samples are visible to the camera. Corrugated paper was obtained at no cost because it was sourced from office waste.

The cuvette used in this study is the standard Hach 2495402 10 mL sample cell with 1-inch square glass for a Hach DR2800 spectrometer, already available in the laboratory. A sample volume of 10 mL was used for each measurement. This amount was adequate for the endoscope to obtain desirable digital images of the samples. If more volume is added into the cuvette, there will not be enough space for the endoscope to enter the cuvette, and the sample could spill over the cuvette.

Table 1 Specification of the digital endoscope used

Features	Specifications
Resolution	1280 x 720/ 640.480 (5.5mm)
Lens diameter	5.5mm
Lamp	Adjustable LED light
Focal length	1.5cm to 2cm
Perspective	70
USB interface	Micro/USB

2.4 The Setup of the Endoscope

The endoscope used in this study was procured from Malaysian online retailer Shopee. It is equipped with a digital camera and six small white LEDs equally spaced in a hexagonal configuration at the tip of the endoscope, to illuminate the samples. Since the position of the camera (detector) is the same as the LEDs (light source), this effectively allows the camera to capture light reflected from water samples. The intensity of light emitted from the LEDs is fixed for the whole measurement. The specification of the endoscope is given in Table 1. The tip of the endoscope is placed just above the surface samples inside the cuvette to allow backscatter light measurement. The endoscope was connected to a personal computer to obtain the images of the samples. An application called "ViewPlayCap" (Figure 4) was installed to allow the computer to communicate with the endoscope. This application allows a user to view the samples in real time, snap images of the samples and save the images in a desired folder for further analysis.
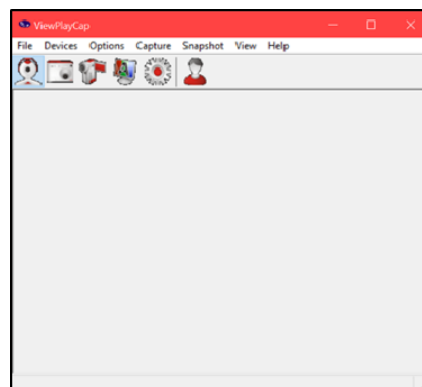

Figure 4 Display of "ViewPlayCap" Software

2.5 Image Processing

A digital endoscope is considered in this study based on the works reported in [12, 15, 28, 29], where digital cameras and image processing were used to determine turbidity of water samples. Images of water samples were obtained from the camera mounted on the tip of the endoscope (Figure 2). Digital images consist of three vector components (u_1, u_2, u_3) for one image pixel (x,y) [30]:

$$C(x,y) = \left(u_1(x,y) + u_2(x,y) + u_3(x,y)\right)^T \quad (2)$$

$$C(x,y) = (u_1, u_2, u_3)^T \quad (3)$$

Quantity u denotes the integer pixel values between 0 and 255. The ranges for map coordinates x and y are $0 \leq x \leq M$ and $0 \leq y \leq N$, where M and N correspond to the resolution of the image, $A = M \times N$. For red-green-blue (RGB) color space, each u corresponds to each color channel:

$$R(x,y) = u_1(x,y) \quad (4)$$

$$G(x,y) = u_2(x,y) \quad (5)$$

$$B(x,y) = u_3(x,y) \quad (6)$$

Only the Red channel is selected due to the color of the dye considered in this study. Vector R is given as:

$$R = \begin{bmatrix} u(1,1) & u(1,2) & \cdots & u(1,n) \\ u(2,1) & u(2,2) & \cdots & u(2,n) \\ \vdots & \vdots & \ddots & \vdots \\ u(m,1) & u(m,2) & \cdots & u(m,n) \end{bmatrix} \quad (7)$$

where each $u(x,y)$ represents each pixel of the image red channel with coordinates x and y as mentioned earlier. The only pixels considered in this study are the ones with a pixel value of 255, which can be interpreted as the "brightest" or "whitest" pixels such that:

$$M = \sum_{j=1}^{i} 255(x,y)_i \quad (8)$$

Theoretically, as the amount of light entering the endoscope increases, it would produce an image with more pixels with a value of 255; hence, the magnitude of M should increase.

3.0 RESULTS AND DISCUSSION

3.1 Absorption and Reflectance of the Dye Samples

Figure 5 shows the absorbance and reflectance of selected dye-water mixture samples between 0.001 g/L and 0.1 g/L red dye concentration. Unfortunately, during the examination, the instrument was not able to detect an absorbance of above 4000 units. As can be seen in Figure 5 (left), the spectrum of the 0.1 g/L sample was not fully displayable (green line). Similar results were also obtained for samples with concentrations higher than 0.1 g/L. For reflectance, it can be observed that the instruments had almost reached the limit of its detection for 0.1 g/L samples. When tested with samples of concentrations higher than 0.1 g/L, similar reflectance plots were obtained.

Despite these results, however, the examination highlights that the absorbances are more significant in the 200-600 nm ranges, and they peak at a range of approximately 510-520 nm before drastically decreasing near 600 nm. The 510-520 nm absorbance peak range is slightly lower than what is reported in other studies (~540 nm) [31]. However, this is still within the green spectrum (490-570 nm), which is expected for red dye UV-Vis light spectra.

On the other hand, the reflectance plot reveals that samples with a low dye concentration (0.001 – 0.005 g/L) reflect most of the light across the visible spectrum (Figure 5). In contrast, samples with a high dye concentration (0.05 – 0.1 g/L) effectively reflect light significantly in the red spectrum (600 – 800 nm). This is expected since, as shown in Figure 1, samples with a low dye concentration are visibly more clear and less "reddish", while samples with a high dye concentration appear much darker and "redder" to naked eyes.

3.2 Analysis of the Sample Images

Images of selected samples taken with the endoscope are shown in Figure 6. The cross markings seen in the images are drawn inside the cabin to guide the user to position the endoscope to be at the centre of the cuvette. The images clearly show that the apparent red intensity of the sample increases with increasing dye concentration, which is already discussed earlier.

Another important observation to note here is the presence of three reflections of the six LEDs of the endoscope; one on the surface of the water samples, and two at the bottom of the glass cuvette, which can be clearly observed in the images as white markings. The white markings on the surface of the water samples appear larger as the red intensity of the samples increases. In contrast, the other white markings do not appear to change significantly with increasing dye concentration. This observation seems to suggest that more light is reflected from the surface of the water samples as dye concentration increases. As reported in [26], the refractive index of dye solution increases with dye concentration. According to Equation (1), as refractive index increases, the reflection increases as well, which can explain the results shown in Figure 6.

3.3 Development of Fitting Models

A total of 26 out of 30 samples with dye concentrations of 0.001- 0.700 g/L were used to develop the statistical relationship between pixel count (M) and measured concentration of red dye solutions. Four samples with dye concentrations of 0.800 – 3.000 g/L could not be included in the model because the results obtained from these samples were not significantly distinguishable from one another.
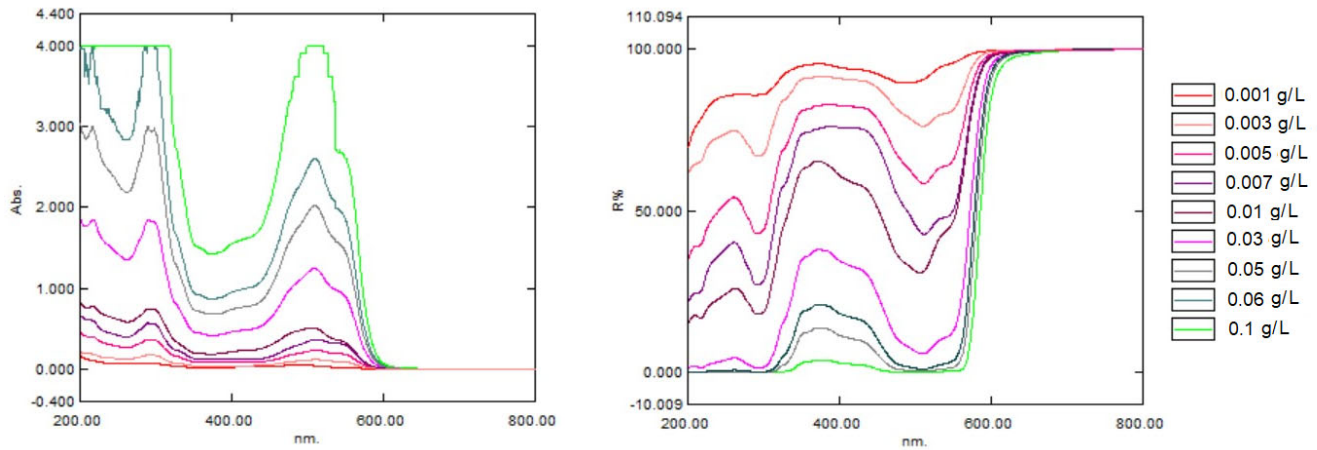
Figure 5 Absorbance (left) and reflectance (right) of selected red dye-water mixture samples
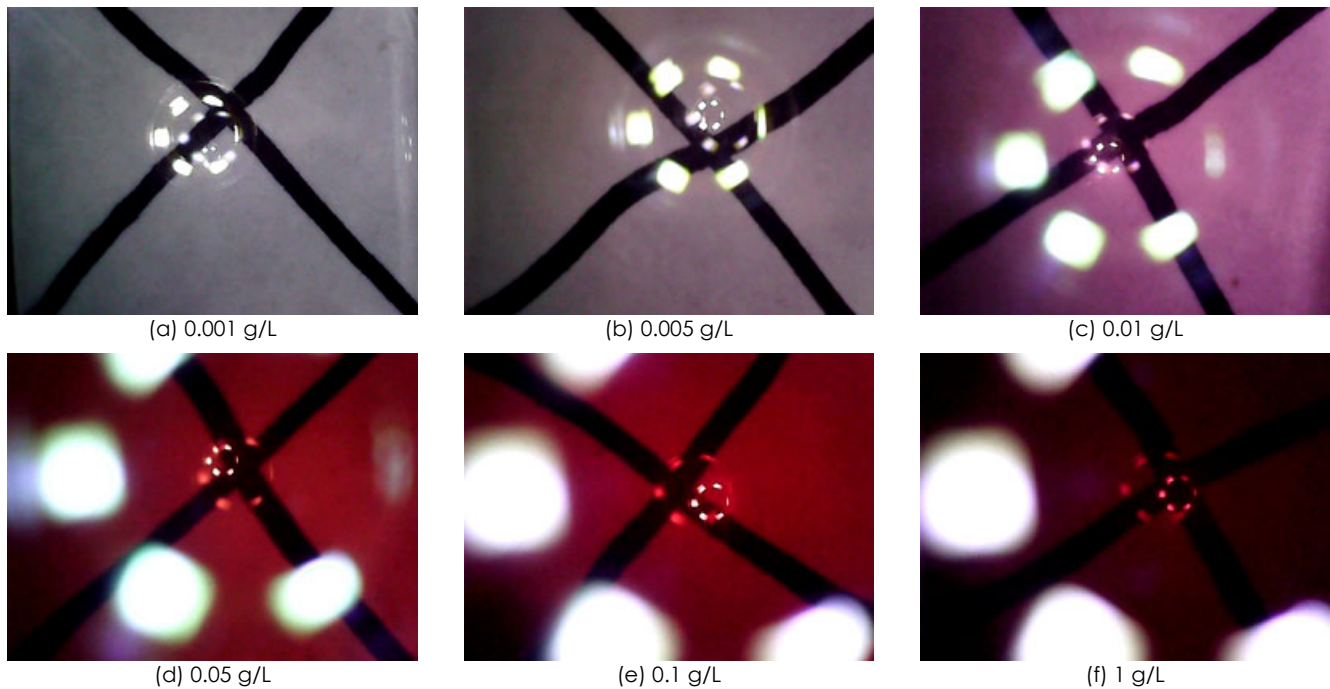

Figure 6 Selected images of dye-water mixture samples taken with endoscope

Figure 7 shows the relationship between pixel count and dye concentration. Three different regression models are developed separately to estimate dye concentration (D.C.) from measured pixel count (M) based on this relationship (Table 2). Note that these three models are needed for three different step-incremental ranges due to the non-linear relationship between pixel count and dye concentration. The reliability of these fitting models is analysed in terms of the coefficient of determination (R^2), root mean square error (RMSE), and normalized RMSE (NRMSE) [32]. The results in Table 2 offer several interpretations:

1. R^2 value, which highlights the predictability of these models and is the most useful indicator according to [33], shows that the third model (0.100 – 0.700 mg/L range) has the best fit, as clearly observed in Figure 7.

2. RMSE emphasizes the significance of the outliers or the errors between predicted and observed values. RMSE seemingly suggests that the third model contains more errors than the other two models. However, this is a little misleading since RMSE fails to take into account the large variance associated with large absolute errors, as discussed in [34].
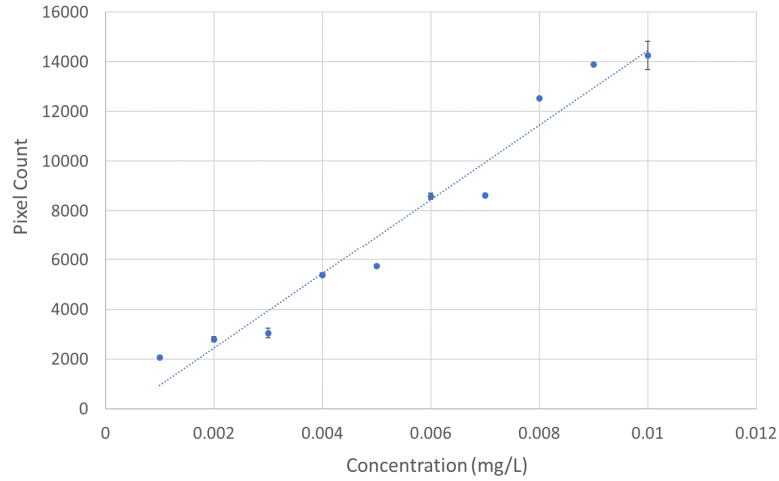
(a) 0.001 g/L – 0.010 g/L range
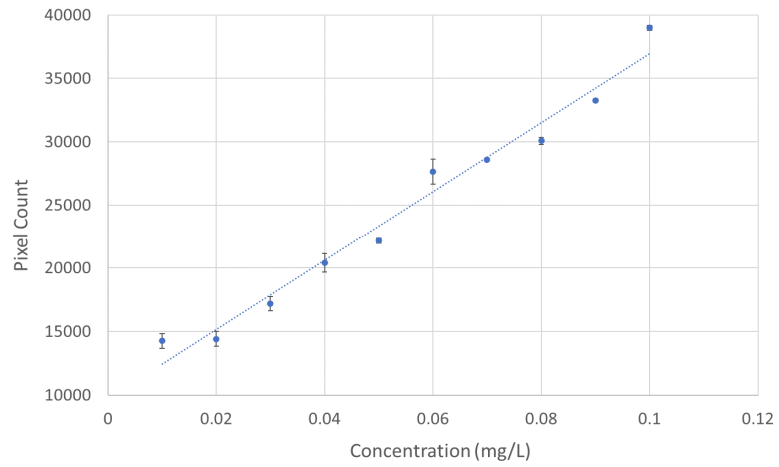
(b) 0.01 g/L – 0.10 g/L
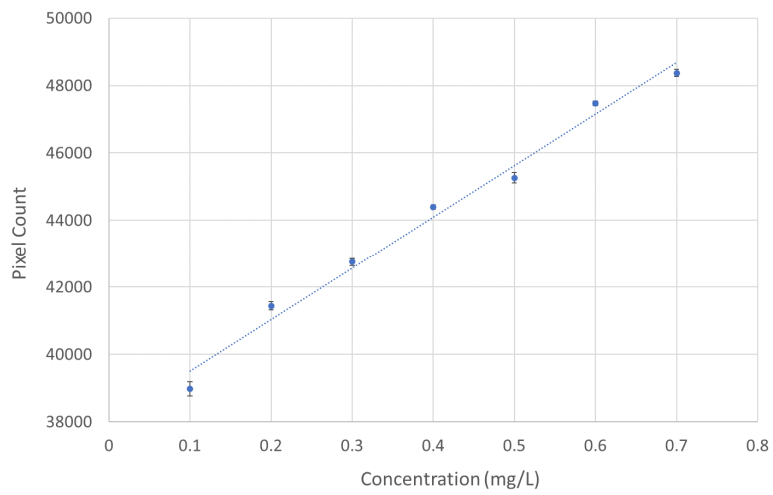
(c) 0.1 g/L – 0.7 g/L

Figure 7 Data fitting for three different ranges of dye concentration

Table 2 The performance of calibration equation relating dye concentration (D.C.) and pixel count (M)

Calibration Equation	Range	Accuracy* (R^2)	RMSE*	NRMSE*
D.C. = (M + 555.44) ÷ 1499026.26	0.001 - 0.010 g/L	0.961	0.001	0.105
D.C. = (M - 9718.00) ÷ 272254.00	0.010 - 0.100 g/L	0.975	0.005	0.083
D.C. = (M - 37988.00) ÷ 15272.00	0.100 - 0.700 g/L	0.987	0.023	0.058

* calculated from [32]

3. Therefore, NMRSE is presented here, which is more suitable than RMSE in accounting for wide observed range of data. NMRSE results shown here are consistent with R^2 values, indicating that the third model is more reliable than the other two models in estimating D.C. from M.

Based on these results, it can be clearly observed that the endoscope is more reliable at determining samples with a higher dye concentration. Omar and MatJafri [24] noted that the backscatter light configuration, as is the case with the endoscope, is less sensitive in detecting a low presence of suspended particles than other configurations. Another reason could possibly be due to the fact that a greater amount of light is reflected to the camera for samples with a higher dye concentration, resulting in better approximation of the concentration of dye.

Even though Chicco *et al*. [33] argues that R^2 = 0.80 indicates a "very good" fitting model, however, at least two recent studies in low-cost optical environmental sensors reported their fitting models as having R^2 values greater than 0.99 [35, 36]. Therefore, more experimental works are necessary to improve the fitting model. This includes repeating the measurements to obtain more data and using sturdier material for the fabrication of the cabin. Employing artificial neural networks (ANN) or convolution neural networks (CNN) is another possibility to improve the fitting model.

In terms of cost, the endoscope used in this study was obtained at a retail price of RM25.00 (~USD6.00). On the other hand, there was no cost incurred for fabricating the cabin, since it was made with paper waste. Some similar studies reported the costs of their systems, while others chose not to disclose such information. For instance, Hoang *et al*. (2021) claimed that their system cost less than USD50.00 [35], while Khoshmaram and Mohammadi (2021) did not provide such information [36]. Therefore, for comparison, the cost of the system in this study is much lesser than that of the system demonstrated in [35].

However, at this point, this study only focuses on the potential application of a low-cost endoscope to be utilized as an optical detector to determine concentration of red dye-water mixture solutions. At this point, no software or mobile application is developed to be used in tandem with the endoscope for conveniences. Even though this idea is considered for future works, the endoscope must be examined further as an optical detection instrument for other types of dyes, analytes, or substances.

4.0 CONCLUSION

This study covers the application of a low-cost digital endoscope and image processing technique in detecting Remazol red dye concentrations in water samples. Three fitting models were developed to detect dye concentrations ranging from 0.001 to 0.700 mg/L. The accuracy of these models is expressed in terms of determination of the coefficients (R2), RMSE, and normalized RMSE. This study demonstrated that a digital endoscope can be utilized as a low-cost light sensor to determine the concentration of Remazol red dye solution, which can be useful in studies involving bioremediation and decolorization of dye waste. Besides dyes, it might also be possible to use the same instrument to detect and determine the presence of other suspended particles in water. However, more experimental work is necessary to explore the potential of digital endoscopes for such applications, especially for different analytes and substances.

References

[1]   Spellman, F. R. 2014. *Handbook of Water and Wastewater Treatment Plant Operations*. Boca Raton: Taylor and Francis Group.
[2]   Surwase, S. V., K. K. Deshpande, S. S. Phugare, and J. P. Jadhav. 2012. Biotransformation Studies of Textile Dye Remazol Orange 3R. *3 Biotech*. 3(4): 267-275. Doi: https://doi.org/10.1007/s13205-012-0093-1.
[3]   Braun, C. L., and S. N. Smirnov. 1993. Why is Water Blue? *Journal of Chemical Education*. 70(8): 612-614. Doi: 10.1021/ed070p612.
[4]   *Guidelines for Drinking-Water Quality*. 1997. Edisi ke-2, Volume 3. World Health Organization. 9.
[5]   Greenberg, A. E., L. S. Clesceri, A. D. Eaton, and M. A. H. Franson. 1992. *Standard Methods for the Examination of Water and Wastewater*. Edisi ke-18. American Public Health Association.

[6] Malakootian, M., and A. Fatehizadeh. 2010. Color Removal from Water by Coagulation/Caustic Soda and Lime. *Iranian Journal of Environmental Health Science and Engineering*. 7(3): 267-272.
URL: http://www.bioline.org.br/pdf?se10030.

[7] Bao, J., T. Li, and B. Ren. 2017. Determination of Wastewater Color by Integral Spectrophotometer based on Complementary Color. *Advances in Engineering Research*. 120: 1249-1253.
Doi: 10.2991/ifeesm-17.2018.228.

[8] Kalantari, M. H., S. A. Ghoraishian, and M. Mohaghegh. 2017. Evaluation of Accuracy of Shade Selection using Two Spectrophotometer Systems: Vita Easyshade and Degudent Shadepilot. *European Journal of Dentistry*. 11(2): 196-200. Doi: 10.4103/ejd.ejd.195.16.

[9] McCracken, K. E., and J-Y. Yoon. 2016. Recent Approaches for Optical Smartphone Sensing in Resource – Limited Settings: A Brief Review. *Analytical Methods*. 8: 6591-6601.
Doi: 10.1039/C6AY01575A.

[10] Zou, L., Z. Gu, and M. Sun, M. 2015. Review of the Application of Quantum Dots in the Heavy-metal Detection. *Toxicology and Environmental Chemistry*. 97: 477-490.
Doi: 10.1080/02772248.2015.1050201.

[11] González-Morales, D., A. Valencia, A. Díaz-Nuñez, M. Fuentes-Estrada, O. López-Santos, and O. García-Beltrán. 2020. Development of a Low-Cost UV-Vis Spectrophotometer and Its Application for the Detection of Mercuric Ions Assisted by Chemosensors. *Sensors*. 20(906): 1-16.
Doi: 10.3390/s20030906.

[12] Ramli, S. N. A., K. Kadaruddin, M. F. Zainuddin and Z. Abbas. 2019. The Development of Low Cost Turbidimeter using Smartphone Camera and Image Processing. *International Journal of Innovative Technology and Exploring Engineering*. 8(8S): 420-424.
URL: https://www.ijitee.org/wp-content/uploads/papers/v8i8s/H10720688S19.pdf.

[13] Gillett, D. and D. Marchiori. 2019. A Low-Cost Continuous Turbidity Monitor. *Sensors*. 19(3039): 1-18.
Doi: 10.3390/s19143039.

[14] Parra, L., J. Rocher, J. Escrivá, and J. Lloret. 2018. Design and Development of Low-cost Smart Turbidity Sensor for Water Quality Monitoring in Fish Farms. *Aquacultural Engineering*. 81: 10-18.
Doi: 10.1016/j.aquaeng.2018.01. 004.

[15] Hussain. I, K. Ahamad and P. Nath .2016. Water Turbidity Sensing using a Smartphone. *RSC Advances*. 6: 22374-22382.
Doi: 10.1039/C6RA02483A.

[16] O'Donoghue, J. 2019. Simplified Low-Cost Colorimetry for Education and Public Engagement. *Journal of Chemical Education*. 96: 1136-1142
Doi: https://doi.org/10.1021/acs.jchemed. 9b00301.

[17] Anzalone, G. C., A. G. Glover and J. M. Pearce. 2013. Open-Source Colorimeter. *Sensors*. 13: 5338-5346.
Doi: 10.3390/s130405338.

[18] Kadaruddin, K. and M. F. Zainuddin. 2020. A Brief Review on Low-cost Turbidimeter Designs. *IOP Conference Series: Earth and Environmental Science*. 476.

[19] Kolekar Y. M. and K. M. Kodam K. M. 2011. Decolorization of Textile Dyes by Alishewanella sp. KMK6. *Applied Microbiology*. 95: 521-529.
Doi: 10.1007/s00253-011-3698-0.

[20] Novotny C., N. Dias, A. Kapanen, K. Malachova, M. Vandrovcova, and M. Itavaara. 2006. Comparative Use of Bacterial, Algal and Protozoan Tests to Study Toxicity of Azo and Anthraquinone Dyes. *Chemosphere*. 63: 1436-1442.
Doi: 10.1016/j.chemosphere.2005.10.002.

[21] Hai, F. I., K. Yamamoto, and K. Fukushi. 2007. Hybrid Treatment System for Dye Wastewater. *Critical Reviews in Environmental Science and Technology*. 37(4): 315-377.

Doi: 10.1080/10643380601174723.

[22] Ekambaram, S. P., Perumal, and U. Annamalai. 2016. Decolorization and Biodegradation of Remazol Reactive Dyes by Clostridium Species. *3 Biotech*. 6(20).
Doi: 10.1007/s13205-015-0335-0.

[23] Gokulan, R., G. G. Prabhu and J. Jegan. 2019. Remediation of Complex Remazol Effluent using Biochar Derived from Green Seaweed Biomass. *International Journal of Phytoremediation*. 21(12): 1-11.
Doi: 10.1080/15226514.2019.1612845.

[24] Omar, A. F. and M. Z. MatJafri. 2009. Turbidimeter Design and Analysis: A Review on Optical Fiber Sensors for the Measurement of Water Turbidity. *Sensors*. 9(10): 8311-8335.
Doi: 10.3390/s91008311.

[25] Reyes-Coronado, A., A. Garcia-Valenzuela, C. Sanchez-Perez, and R. G. Barrea. 2005. Measurement of the Effective Refractive Index of a Turbid Colloidal Suspension using Light Refraction. *New Journal of Physics*. 7(89): 1-21.
Doi: 10.1088/1367-2630/7/1/089.

[26] Zhang, X., D. J. Faber, A. L. Post, T. G. van Leeuwen, and H. J. C. M. Sterenborg. 2019. Refractive Index Measurement using Single Fiber Reflectance spectroscopy. *Journal of Biophotonics*. 12(7): 1-11.
Doi: 10.1002/jbio.201900019.

[27] Sai, T., M. Saba, E. R. Dufresne, U. Steiner, and B. D. Wilts. 2020. Designing Refractive Index Fluids using the Kramers–Kronig Relations. *Faraday Discussion*. 223: 136-144.
Doi: 10.1039/D0FD00027B.

[28] Hamidi, F. N., M. F. Zainuddin, Z. Abbas, and A. F. Ahmad. 2017. Low Cost and Simple Procedure to Determine Water Turbidity with Image Processing. *International Conference on Imaging, Signal Processing and Communication (ICISPC) 2017*. Penang, Malaysia. 26 – 28 July 2017. 30-34.
Doi: 10.1145/3132300.3132302.

[29] Karnawat, V. and S. L. Patil. 2016. Turbidity Detection using Image Processing. *International Conference on Computing, Communication and Automation (ICCCA) 2016*. Uttar Pradesh, India. 29-30 April 2016): 1086-1089.
Doi: 10.1109/CCAA.2016.7813877.

[30] Koschan, A. and M. Abidi. 2008. *Digital Color Image Processing*. New Jersey: John Wiley and Sons, Inc.

[31] Malkoc, S. 2017. Removal of Remazol Red Dye with Live Cell Aspergillus Terreus. *Anadolu University Journal of Science and Technology A- Applied Sciences and Engineering*. 18(3): 654- 662.
Doi: 10.18038/aubtda.283045.

[32] AgriMetSoft. 2019. Online Calculators. Available on:vhttps://agrimetsoft.com/calculators/Normalized%20Root%20Mean%20Square%20Error. Last assessed: 18 Disember 2021.

[33] Chicco, D., M. J. Warrens, and G. Jurman. 2021. The Coefficient of Determination R-squared is More Informative than SMAPE, MAE, MAPE, MSE and RMSE in Regression Analysis Evaluation. *Peer J Computer Science*. 7:e623: 1-24.
Doi: 10.7717/peerj-cs.623.

[34] Chai, T. and R. R. Draxler. 2014. Root Mean Square Error (RMSE) or Mean Absolute Error (MAE)? – Arguments against Avoiding RMSE in the Literature. *Geoscience Model Development*. 7: 1247-1250.
Doi: 10.7717/peerj-cs.623.

[35] Hoang, L. Q., H. B. L. Chi, D. N. N. Khanh, N. T. T. Vy, P. X. Hanh, T. N. Vu, H. T. Lam, and N. T. K. Phuong. 2021. Development of a Low-cost Colorimeter and its Application for Determination of Environmental Pollutants, *Spectrochimica Acta Part A: Molecular and Biomolecular Spectroscopy*. 249: 119212.
Doi: 10.1016/j.saa.2020.119212.

[36] Khoshmaram, L. and M. Mohammadi. 2021. Combination of a Smart Phone based Low-cost Portable Colorimeter with Air-assisted Liquid-liquid Microextraction for Speciation and Determination of Chromium (III) and (VI). *Microchemical Journal*. 164(105991).
Doi: 10.1016/j.microc.2021.105991.